Journal of Zhejiang University-SCIENCE A (Applied Physics & Engineering)
ISSN 1673-565X (Print); ISSN 1862-1775 (Online)
www.jzus.zju.edu.cn; www.springerlink.com
E-mail: jzus@zju.edu.cn

Influence of annealing conditions on the properties of $Cu(In,Ga)Se_2$ thin films fabricated by electrodeposition*

Jing-yu QU, Zheng-fei GUO, Kun PAN, Wei-wei ZHANG, Xue-jin WANG†‡

College of Science, China Agricultural University, Beijing 100083, China

†E-mail: xjwang@cau.edu.cn

Received May 16, 2017; Revision accepted July 27, 2017; Crosschecked Apr. 11, 2018

Abstract: $Cu(In,Ga)Se_2$ (CIGS) precursor films were deposited on Mo/glass by electrodeposition, and then annealed in Se vapor. The annealing temperature ranged from 450 °C to 580 °C, and two heating rates were selected. The results showed that the crystalline quality of the CIGS films and formation of the Cu-Se compound could be strongly influenced by the selenization temperature and heating rate. Raman spectroscopy and X-ray diffraction (XRD) analysis showed that when the selenization temperature was increased from 450 °C to 550 °C, the amount of binary CuSe phase decreased and the amount of Cu_2Se increased. After annealing at 580 °C, a minimum amount of $Cu_{2-x}Se$ compounds was obtained and the degree of CIGS film crystallinity was higher than in other samples. The relationship between the properties of the film and the heating rate was studied. XRD and Raman spectra showed a decrease in the $Cu_{2-x}Se$ phase with increasing heating rate. Scanning electron microscopy (SEM) and XRD showed a remarkable increase in the grain size of CIGS during rapid heating.

Key words: $Cu(In,Ga)Se_2$ (CIGS) thin films; Electrodeposition; Selenization; Raman spectroscopy
https://doi.org/10.1631/jzus.A1700261 **CLC number:** O47; O64

1 Introduction

Solar cells are photoelectric conversion devices which have attracted the attention of researchers for some time (Chen et al., 2017). Among different kinds of solar cells, $Cu(In,Ga)Se_2$ (CIGS) thin film solar cells have many advantages, such as high efficiency, low cost, and long term stability (Sebastian et al., 1999). They have an extraordinarily high absorption coefficient of 1×10^5 cm^{-1} (Hamakawa, 2012), and in view of its direct bandgap, CIGS will become a substitute for silicon solar cells. $CuInSe_2$ (CIS) and $CuGaSe_2$ have bandgap energies of 1.02 eV and 1.68 eV, respectively (Birkmire and Eser, 1997), so the bandgap of chalcopyrite CIGS is changed by substituting indium for gallium.

Over the years, the improvement of the quality of CIGS thin films has been the key to increasing the efficiency of solar cells. A variety of methods such as co-evaporation (Powalla et al., 2009; Chen et al., 2013), electrodeposition (Friedfeld et al., 1999; Ao et al., 2009; Malaquias et al., 2015), chemical bath deposition (Bhattacharya et al., 1998), and sputtering (Zhang and Hong, 2016) have generally been used for preparing CIGS thin films. The most efficient solar cells have been fabricated by the method of co-evaporation (Jackson et al., 2014). However, this technique is relatively expensive due to high equipment costs and loss of metal vapors on surfaces unrelated to photovoltaic module production. The fabrication of CIGS thin films by electrodeposition is an attractive method because of its use of low-cost

‡ Corresponding author
* Project supported by the National High-Tech R&D Program (863 Program) of China (No. 2015AA034201), the National Natural Science Foundation of China (No. 11474355), and the Chinese Universities Scientific Fund (No. 2017LX002)
ORCID: Jing-yu QU, https://orcid.org/0000-0003-4996-2625

equipment and its suitability for manufacturing large-area polycrystalline films (Harati et al., 2010; Saji et al., 2011; Yeh et al., 2016). In the processing of selenium-deficient CIGS precursor films deposited by electrodeposition, a thermal treatment in a Se atmosphere can improve the stoichiometry and morphology of the electrodeposited thin films. Electrodeposited films may be amorphous, with the presence of some binary phase like Cu-Se or In-Se compounds (Lincot et al., 2004). As such, an annealing process is necessary (Yamanaka et al., 1991; Lakshmikumar and Rastogi, 1996). Currently, the favoured method of selenization uses H_2Se which produces a high quality CIGS film (Basol and Kapur, 1990). Unfortunately, H_2Se is poisonous, flammable, and difficult to store and handle. Selenium powder can be used as a solid selenium source as it needs no complicated devices, hazardous operations, and strict control conditions. There are still many outstanding technical and scientific issues regarding the process of selenization and its correlation to the quality of CIGS precursor films fabricated by electrodeposition. There have been few reports about the effect of annealing conditions on electrodeposited $Cu(In,Ga)Se_2$ thin films.

In this study, CIGS precursor films were fabricated by electrodeposition and then the effects of selenization temperatures and heating rates on the properties of the films were investigated. X-ray diffraction (XRD) spectra, scanning electron microscopy (SEM), and Raman scattering spectroscopy were used to investigate the components and structure of the films under different conditions.

2 Experimental

Mo films were deposited onto soda-lime glass substrates by sputtering. The thickness of the Mo layers was about 600 nm. Before CIGS film coating, the Mo/glass substrates were cut into 3 cm×2 cm square pieces and cleaned in alcohol and hydrochloric acid to remove surface oil stain and oxide. The electrodeposition bath contained $CuCl_2$ (6 mmol/L, 99.0%), $InCl_3$ (21.24 mmol/L, 99.99%), $GaCl_3$ (10 mmol/L, 99.99%), and H_2SeO_3 (1.5 mmol/L). Instead of sodium citrate, 20 mmol/L of triethanolamine was used as a complexing agent to increase the Ga concentration in the CIGS precursor films. We also compared the effects of other agents, such as sodium citrate and sodium sulfamate, but we chose triethanolamine as the complexing agent because its use made it easier to deposit Ga. NaCl was added to increase the conductivity of the solution during electrodeposition. The final pH was adjusted to 3.25 with dilute hydrochloric acid.

Deposition of CIGS thin films was performed in potentiostatic mode, using an electrochemical workstation (AUTOLAB PGSTAT302N, Switzerland), at room temperature and without stirring. The film was first deposited at a potential of −0.7 V (vs. saturated calomel electrode (SCE)) for 1800 s, followed by a deposition process at −1.08 V (vs. SCE) for 450 s. After electrodeposition, the CIGS precursor films were rinsed with deionized water and dried with nitrogen gas. Then the electrodeposited thin films were annealed with Se vapor in a furnace. The samples were placed in the middle of a graphite box. Se powder was placed in each of the two ends of the box, which was placed inside a large tube to maintain Se vapor pressure during heating. The graphite box was covered to keep an adequate concentration of Se, but was not sealed. The working pressure during annealing remained at 4000 Pa using nitrogen to maintain an oxygen-free atmosphere. Before heating, the tube was purged three times with high purity nitrogen.

First, the selenization temperature was varied from 450 °C to 580 °C with an isothermal duration of 1 h. As soda-lime glass substrates warp at temperatures of 600 °C, 580 °C was selected as the highest selenization temperature. The heating rate was 55 K/min. Second, the influence of the ramp rates during selenization on the structural properties of CIGS was investigated. Two ramp rates were performed, 55 K/min and 550 K/min, followed by a thermal treatment of 550 °C for 1 h.

The composition of the thin films was examined by X-ray fluorescence (XRF, Fischerscope X-ray XDV SDD, Germany). The surface morphology and cross-sectional micrographs of the samples were observed by field emission scanning electron microscopy (FE-SEM, Hitachi, S-5200, Japan). The structural characterization and crystallinity values of the CIGS thin films were tested by X-ray diffraction (D/MAX-YB diffractometer (Japan) with Cu-$K_{\alpha 1}$

radiation, λ=1.5406 Å). Raman spectra were recorded using a Princeton Instruments spectrometer (model Acton SP2500, USA) in backscattering configuration with a He-Ne 633 nm laser line. The excitation power on the sample was about 20 mW.

3 Results and discussion

Table 1 shows the chemical composition of the CIGS precursor film deposited on bare soda-lime glass and films selenized at different temperatures for 1 h. The Cu/(In+Ga) ratio was 0.83 and the Ga/(In+Ga) ratio 0.23 in the surface region of the CIGS film before annealing. The experiment was repeated. For each electrodeposited film, the same experimental conditions were maintained. Using XRF, the error of the metal precursor ratio for different samples was less than 0.01. The selenium content of the precursor films was not optimized because selenium was subsequently added in the selenization process. Increasing the temperature of selenization caused the Cu/(In+Ga) and Ga/(In+Ga) ratios to increase slightly. This result suggests that In and Ga compounds evaporated when the annealing was performed at high temperature. Moreover, the Se concentration of the precursor film increased noticeably after selenization, suggesting that the selenium composition of the film is dominated by the selenization process. Many researchers have found that CIGS absorbers with high photovoltaic conversion efficiency have an atomic ratio of 0.88<Cu/(In+Ga)<0.95 and Ga/(In+Ga)≈0.3 (Contreras et al., 2006). The results in Table 1 coincide with the above atomic ratio range of high quality CIGS films.

The purpose of adding the Se to the precursor is to improve the degree of crystallinity. To understand the effect of Se content on the properties of CIGS films, precursor baths containing various concentrations of H_2SeO_3 were prepared, with all other conditions held constant. After annealing all the samples, the crystalline properties of the films were evaluated by XRD and SEM. The concentrations of H_2SeO_3 in the ion bath were (a) 3 mmol/L, (b) 6 mmol/L, and (c) 9 mmol/L (Fig. 1). A lower degree of recrystallization was achieved as the concentration of H_2SeO_3 in the ion bath increased. Some cracks even appeared when H_2SeO_3 increased to 9 mmol/L. The samples were analyzed with the XRD (Fig. 1). In Fig. 1d, all the samples clearly show the diffraction peaks characteristic of chalcopyrite phase associated with (112), (204/220), and (312/116) reflections. As the concentration of H_2SeO_3 increased, the diffraction peak intensity decreased and the full width at half-maximum (FWHM) became narrower, indicating a decreasing degree of crystallinity.

We conclude that too much H_2SeO_3 will reduce the quality of CIGS films. Fernandez and Bhattacharya (2005) also found that too much H_2SeO_3 may cause cracks on the surface of films.

Deposition of the CIGS with no Se present in the bath was also attempted, but failed as the H_2SeO_3 in the buffer is a necessary component. A key point of the proposed deposition mechanism, which is widely accepted, is that the composition of the film is controlled by the ratio between selenium and copper fluxes to the electrode. This in turn controls the insertion of indium by the Krogers mechanism (Panicker et al., 1978) between excess selenium in the copper selenide film and indium ions. The standard reduction potential values of Se^{4+}/Se, Cu^{2+}/Cu, In^{3+}/In, and Ga^{3+}/Ga are +0.740 V, +0.342 V, −0.338 V, and −0.523 V vs. standard hydrogen electrode (SHE), respectively. Therefore, Se and Cu are rather easily deposited, but In and Ga are more difficult due to the rather negative values. Se induced the underpotential deposition of both Cu^{+} and In^{3+} and thus the

Table 1 Chemical composition results (tested by XRF) for precursor films and selenized films as a function of selenization temperature

Item	Atomic percentage (%)				Ratio	
	Cu	In	Ga	Se	Cu/(In+Ga)	Ga/(In+Ga)
Precursor film	44	41	12	3	0.83	0.23
CIGS (at 450 °C)	24	21	6	49	0.92	0.22
CIGS (at 500 °C)	25	21	6	48	0.93	0.22
CIGS (at 550 °C)	25	20	6	49	0.96	0.23
CIGS (at 580 °C)	25	19	6	50	1.00	0.24

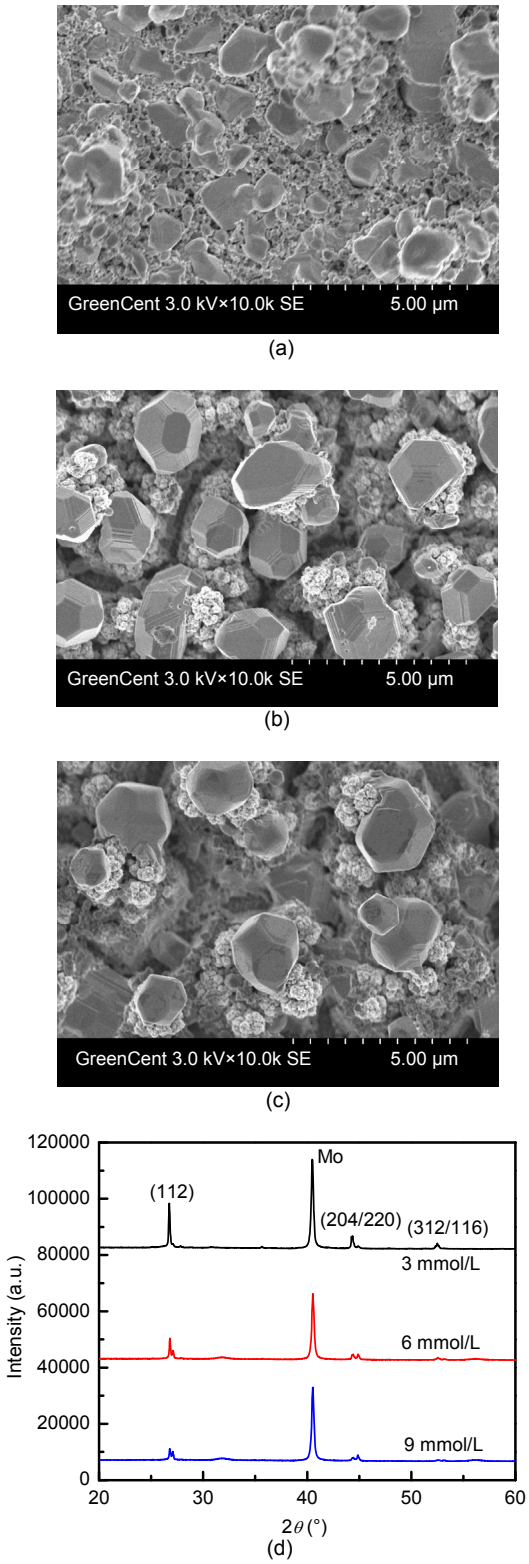

Fig. 1 SEM images of CIGS recrystallization as a function of the concentration of H_2SeO_3
(a) 3 mmol/L; (b) 6 mmol/L; (c) 9 mmol/L; (d) XRD patterns of the above three CIGS films

simultaneous formation of Cu_xSe and In_xSe (Lincot et al., 2004). The Krogers mechanism has been evidenced in other study (Kemell et al., 2000).

The XRD patterns of the CIGS thin films deposited and annealed at different temperatures (isothermal time of 1 h) in Se vapor are shown in Fig. 2. Detailed structural properties of the film can be inferred from peak symmetry and FWHM. Fig. 2 shows that the XRD patterns of the annealed films at various temperatures are almost the same. In all the patterns, the samples exhibit strong preferential orientation at the (112), (204/220), and (312) planes, with corresponding peaks situated at 26.83°, 44.43°, and 52.67°, respectively. The three main diffraction peaks can be attributed to the CIGS chalcopyrite structure. No peaks of chalcopyrite CIGS or CIS were found in the XRD pattern of precursor films in this study before selenization, but two small peaks centered at 2θ= 34.52° and 43.06° correspond to the (200) and (−134) planes of CuIn (JCPDS No. 35-1150). Karg et al. (1993) also found Cu-In phase in precursors. An additional peak at 2θ=40.52° can be attributed to Mo (110). We conclude from this set of data that the crystallinity of electrodeposited films is low. For the samples selenized at 450 °C and 500 °C for 1 h, an additional weak peak centered at 2θ=30.82° appeared, corresponding to CuSe (006) (JCPDS No. 86-1240). Considering that some diffraction peaks characteristic of $Cu_{2-x}Se$ overlap some diffraction peaks of CIGS, the $Cu_{2-x}Se$ phase may have existed when samples were heated at relatively low temperatures. With increasing selenization temperature, the intensity of the diffraction peak centered at 30.82° decreased, which is indicative of a reduction in the content of CuSe. This phenomenon was also found by Zhang et al. (2010). When annealed at 450 °C, the intensity of the (112), (204/220), and (312) peaks was the strongest, and the FWHM of the film was greater than that at other temperatures, which is indicative of a higher degree of crystallization and a smaller grain size. Because the $Cu_{2-x}Se$ compound and chalcopyrite CIGS have a similar structure, all $Cu_{2-x}Se$ Bragg reflections coincide with the reflections of chalcopyrite. The strong intensity of the (112), (204/220), and (312) diffraction peaks may have resulted from the superposition of the peaks of CIGS and $Cu_{2-x}Se$. When the annealing temperature increased from 500 °C to 580 °C, the intensity of the diffraction peaks

of chalcopyrite became stronger, indicating a more crystalline material. Using XRD alone, it was difficult to determine if Cu-Se compounds were present in the CIGS film. Raman scattering was adopted due to its sensitivity to the presence of structural defects, stress or binary phases, which can significantly affect the crystallinity (Izquierdo-Roca et al., 2009).

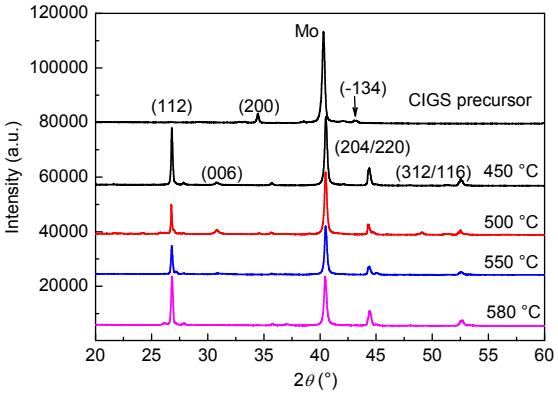

Fig. 2 XRD patterns of CIGS precursor and CIGS films selenized at different temperatures for 1 h

Raman spectra of CIGS films annealed at various selenization temperatures for 1 h are shown in Fig. 3. The Raman detection depth was estimated to be between 100 and 200 nm because of the laser penetration length and the large absorption coefficient of CIGS. For all the samples, the Raman spectra exhibited clear peaks at 179 cm^{-1} and 212 cm^{-1}, which can be attributed to the chalcopyrite A_1 and B_2/E modes, respectively, of the CIGS compound (Delsol et al., 2004). A_1 mode corresponds to the motion of the Se atoms, and B_2/E mode results from the combined vibrations of all the atoms. The values of the frequency of the chalcopyrite A_1 mode for the CIGS films were higher than those for pure CIS (173 cm^{-1}) because Ga was present. The A_1 mode frequency increased linearly as the Ga content increased (Friedfeld et al., 1999; Witte et al., 2006) because CIGS has a smaller bond length than CIS, which may cause a slight blue-shift in wave number. For the CIGS film annealed at 450 °C, an additional peak centered at 237 cm^{-1} was detected, attributable to the formation of In_2Se_3 (Mise and Nakada, 2009). The A_1 mode of CIGS at 179 cm^{-1} and the peak at 212 cm^{-1} narrowed with increasing annealing temperature suggesting an improvement in CIGS film crystallinity. Increasing annealing temperature also caused the intensity of the 260 cm^{-1} peak to increase. This peak was assigned to the A_1 mode of the Cu-Se phase, like Cu_2Se and CuSe (Witte et al., 2008). However, the 260 cm^{-1} peak almost disappeared when the selenization temperature rose to 580 °C. It is clear that the crystallinity of the $Cu_{2-x}Se$ phase improved with increasing annealing temperature, except for a decrease at 580 °C. The overall trend could be explained by a phase segregation caused by inadequate reaction for the films at low selenization temperatures. While annealing at 580 °C, adequate diffusion of atoms induced the formation of quaternary phase and the disappearance of binary phase. Therefore, by annealing at 580 °C, the intensity of peaks corresponding to the A_1 and B_2 modes of CIGS increased, and the other phases, such as $Cu_{2-x}Se$, were depleted.

Table 1 indicates that in general atomic percentage of Se increased as the selenization temperature increased. Sufficient Se was incorporated into the precursor at selenization temperatures of up to 580 °C. This suggests that the higher selenization temperature accelerated Se incorporation (Jiang and Feng, 2006). Selenized precursors, at different temperatures, can be thought of as the part of the selenization process. Raman and XRD data show the reduction of the $Cu_{2-x}Se$ and In_2Se_3 phases with increasing temperature. This can be interpreted as follows: Se diffuses into precursors, and reacts with Cu-In or other amorphous metal to form $Cu_{2-x}Se$ and In_2Se_3. The peaks belonging to CIGS indicate a reaction between the selenides: $Cu_{2-x}Se+In_2Se_3 \rightarrow CuInSe$. Simultaneously, liquid or quasi liquid Ga displaces some In in CIS. The growth of the grain can be analyzed from the plan-view SEM micrographs of selenized films.

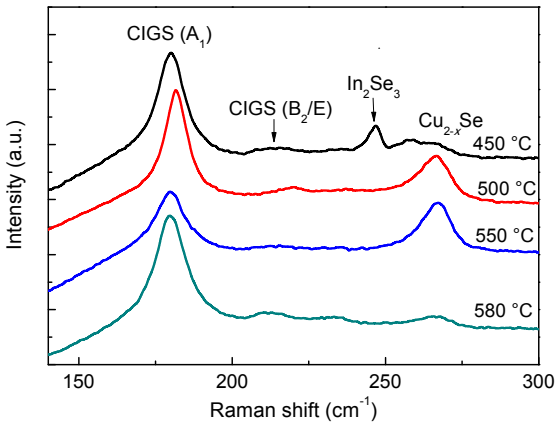

Fig. 3 Raman spectra of CIGS films selenized at different temperatures for 1 h

SEM images (magnification 10000×) of the electrodeposited film and CIGS films annealed at different temperatures are illustrated in Fig. 4. In Fig. 4a, cauliflower-like grains and a multinuclear crystalline structure are observed on the surface prior to annealing. After selenization, the surface morphology became more even and smooth. In Fig. 4b, after annealing at 450 °C, the film was not compact, but the grains on the surface were large. At 500 °C (Fig. 4c), the grain size increased further and the surface of the film was uniform and smooth. However, defects and surface pinholes were still observed. In Fig. 4d, at 550 °C, the CIGS film had a compact and fine-grained dense surface, with few defects observed. When the heating temperature was increased to 580 °C, no surface pinholes were observed (Fig. 4e). The results confirm that the surface morphology of CIGS films seems sensitive to the annealing temperature. After annealing under a constant Se vapor pressure, the CIGS films became denser and the cauliflower-like multinuclear grains were eliminated. The surface morphology was improved. It is clear that defects and pinholes disappeared with increasing annealing temperature. These defects act as recombination centers and are known to decrease the open circuit voltage (Voc) and fill factor (FF) of solar cells (Rau and Schock, 1999). The rough surface structure in Figs. 4b and 4c confirms that the reaction and recrystallization process had not been fully concluded. Increasing the selenization temperature to 580 °C made obvious improvements to the crystal structure that were easily detected. The role of Cu_xSe cannot be ignored since most reports in the literature have concentrated on the use of Cu selenides as a precursor for attaining good quality films with improved crystal sizes (Adurodija et al., 1999).

Table 2 shows the chemical composition of samples obtained by annealing under two different heating rates. The ratio of Cu/(In+Ga) decreased during fast annealing, bringing it closer to the atomic ratio of high quality CIGS. The ratio of Ga/(In+Ga) was almost the same after annealing using a different heating rate. We conclude that fast annealing could prevent the evaporation of indium and gallium compounds.

The evolution of the CIGS under different heating rates is shown in Fig. 5. From the XRD patterns, it can be seen that there was little difference between the compositions of the CIGS films, reflections (112), (220), and (312) related to chalcopyrite. As the heating rate increased, the intensity of the diffraction peaks at 2θ=26.83°, 44.43°, and 52.67°

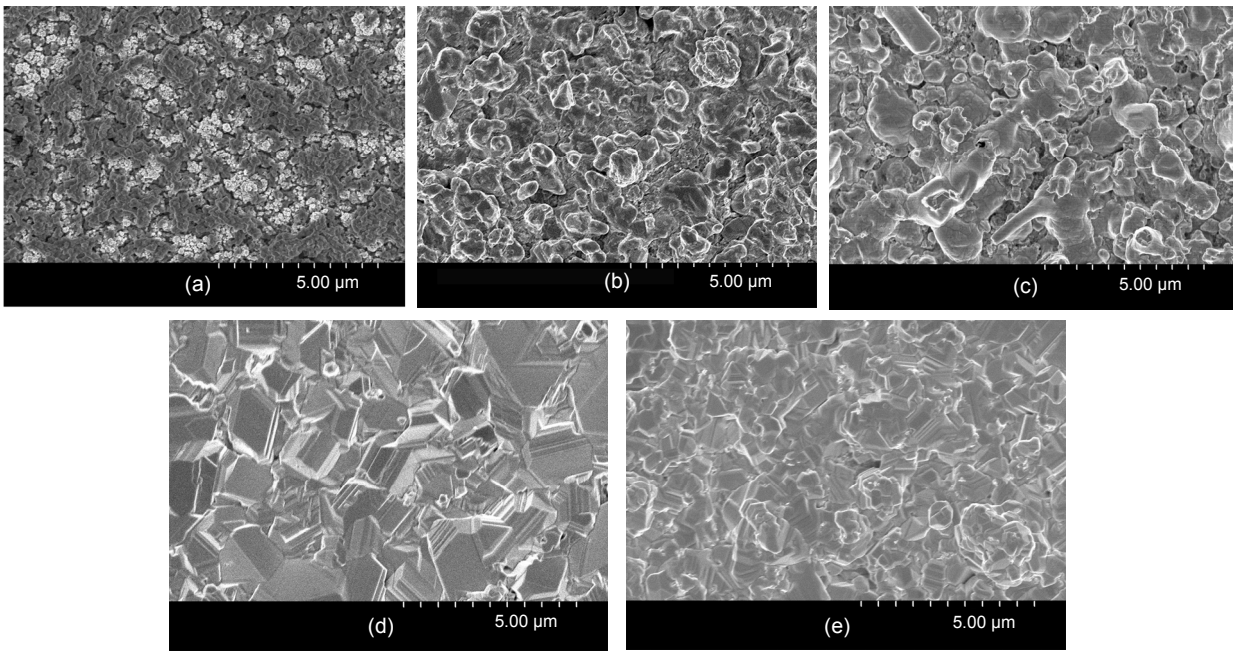

Fig. 4 SEM images of CIGS precursor and films selenized at different temperatures
(a) Precursor; (b) 450 °C; (c) 500 °C; (d) 550 °C; (e) 580 °C

Table 2 Chemical composition results (tested by XRF) for precursor films and selenized films as a function of heating rates

Item	Atomic percentage (%)				Cu/(In+Ga) ratio
	Cu	In	Ga	Se	
Precursor film	44	41	12	3	0.83
Heating rate of 55 K/min	25	20	6	49	0.96
Heating rate of 550 K/min	25	23	6	46	0.84

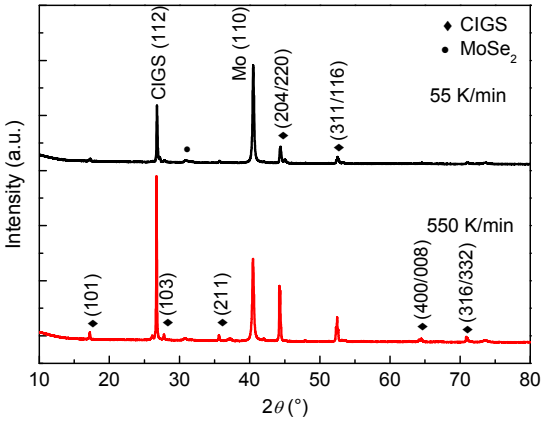

Fig. 5 XRD patterns of CIGS films selenized at 550 °C for 1 h at different heating rates

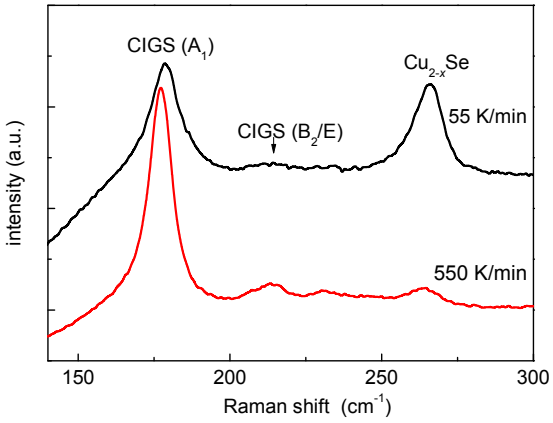

Fig. 6 Raman spectra of CIGS films selenized at 550 °C for 1 h at different heating rates

increased, corresponding to the (112), (220), and (312) planes, respectively, of the CIGS chalcopyrite structure. The FWHM of these three peaks decreased when the heating rate was high, which could be attributed to the growth of grain. In addition, when the sample was heated to 550 °C in 1 min, some peaks with low intensity, such as the (101), (103), (211), (400/008), and (316/332) peaks, were obtained in the XRD pattern, corresponding to chalcopyrite CIGS. Based on the XRD patterns of the two samples obtained by annealing at different heating rates, we conclude that fast annealing is propitious to the growth of grain and an increase in crystallinity.

The Raman spectra of the CIGS thin films obtained by annealing at different heating rates are shown in Fig. 6. The Raman peak located at 179 cm^{-1} corresponds to the A_1 mode of CIGS, whilst the peak at 212 cm^{-1} corresponds to the B_2 or E mode of CIGS. An additional peak at 260 cm^{-1} can be attributed to the $Cu_{2-x}Se$ compound. For samples subjected to fast annealing, the A_1 and B_2/E modes of CIGS were narrower than those annealed at the lower heating rate. In addition, the intensity at 260 cm^{-1} decreased, and the peak became narrower, indicating that fast annealing prevents the formation of $Cu_{2-x}Se$.

SEM images of the CIGS thin films obtained by annealing under different heating rates are shown in Fig. 7. During conventional annealing, the CIGS film had a flake shaped surface, and no defects or pinholes were deserved (Fig. 7a). The film was uniform and compact. With increasing heating rate, the grain size increased and the surface consisted of angular crystallites (Fig. 7b). The crystallinity of the film was higher.

4 Conclusions

In this study, CIGS precursors were synthesized by electrodeposition, with subsequent annealing in a Se atmosphere to improve crystal quality. The annealing temperature ranged from 450 °C to 580 °C and two heating rates were selected. The CIGS films were then examined by XRF, SEM, XRD, and Raman scattering. The ratios of Cu/(In+Ga) and Ga/(In+Ga) increased with elevated selenization temperature,

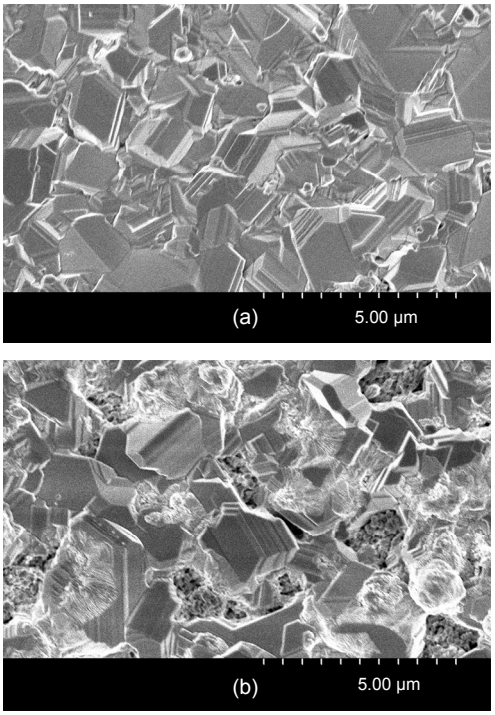

Fig. 7 SEM images of CIGS films selenized at 550 °C for 1 h with different heating rates
(a) 55 K/min; (b) 550 K/min

which reveals that compounds containing indium and gallium may be evaporated when the annealing temperature is high. XRD analysis showed that CIGS crystals are formed in the selenization process. As the annealing temperature increased from 450 °C to 550 °C, the improvement of film crystallinity was due to the increase of the Cu_2Se phase, but the amount of binary Cu-Se phase decreased, as inferred from Raman scattering and XRD analysis. After annealing at 580 °C, minimum amounts of $Cu_{2-x}Se$ compounds were obtained and the degree of CIGS film crystallinity was higher than in other samples. The film was compact and no pinholes were detected in the SEM images. The samples treated at the high heating rate had a slightly lower ratio of Cu/(In+Ga) than samples treated at the low heating rate. The ratio of Ga/(In+Ga) remained unchanged, which illustrates that fast heating could prevent the evaporation of indium and gallium compounds. XRD and Raman scattering indicated that the crystallinity of the films improved noticeably with increasing heating rate and caused the grain size to become larger, which was consistent with the observed SEM image. This study revealed the effects of selenization temperature and heating rate on the properties of CIGS films.

Acknowledgements

The authors thank Prof. Leo WM LAU and Dr. Cheng LIAO (Chengdu Green Energy and Green Manufacturing Technology R&D Centre, Chengdu Development Center of Science and Technology, China) for their technical and experimental supports, and thank China Academy of Engineering Physics for suggestion about the study.

References

Adurodija FO, Song J, Kim SD, et al., 1999. Growth of $CuInSe_2$ thin films by high vapour Se treatment of co-sputtered Cu-In alloy in a graphite container. *Thin Solid Films*, 338(1-2):13-19. https://doi.org/10.1016/S0040-6090(98)00358-7

Ao JP, Yang L, Yan L, et al., 2009. Comparison of the compositions and structures of electrodeposited Cu-poor and Cu-rich $Cu(In_{1-x}Ga_x)Se_2$ films before and after selenization. *Acta Physica Sinica*, 58(3):1870-1878.

Basol BM, Kapur VK, 1990. Deposition of $CuInSe_2$ films by a 2-stage process utilizing e-beam evaporation. *IEEE Transactions on Electron Devices*, 37(2):418-421. https://doi.org/10.1109/16.46376

Bhattacharya RN, Batchelor W, Granata JE, et al., 1998. $CuIn_{1-x}Ga_xSe_2$-based photovoltaic cells from electrodeposited and chemical bath deposited precursors. *Solar Energy Materials and Solar Cells*, 55(1-2):83-94. https://doi.org/10.1016/S0927-0248(98)00049-X

Birkmire RW, Eser E, 1997. Polycrystalline thin film solar cells: present status and future potential. *Annual Review of Materials Science*, 27(1):625-653. https://doi.org/10.1146/annurev.matsci.27.1.625

Chen CH, Hu HT, Lin FM, et al., 2017. Residual stress analysis and bow simulation of crystalline silicon solar cells. *Journal of Zhejiang University-SCIENCE A (Applied Physics & Engineering)*, 18(1):49-58. https://doi.org/10.1631/jzus.A1500279

Chen DS, Yang J, Xu F, et al., 2013. Performance improvement of CdS/$Cu(In,Ga)Se_2$ solar cells after rapid thermal annealing. *Chinese Physics B*, 22(1):018801. https://doi.org/10.1088/1674-1056/22/1/018801

Contreras MA, Romero MJ, Noufi R, 2006. Characterization of $Cu(In,Ga)Se_2$ materials used in record performance solar cells. *Thin Solid Films*, 511-512:51-54. https://doi.org/10.1016/j.tsf.2005.11.097

Delsol T, Samantilleke AP, Chaure NB, et al., 2004. Experimental study of graded bandgap $Cu(InGa)(SeS)_2$ thin films grown on glass/molybdenum substrates by selenization and sulphidation. *Solar Energy Materials and Solar Cells*, 82(4):587-599. https://doi.org/10.1016/j.solmat.2004.02.018

Fernandez AM, Bhattacharya RN, 2005. Electrodeposition of $CuIn_{1-x}Ga_xSe_2$ precursor films: optimization of film composition and morphology. *Thin Solid Films*, 474(1-2):

10-13.
https://doi.org/10.1016/j.tsf.2004.02.104

Friedfeld R, Raffaelle RP, Mantovani JG, 1999. Electrodeposition of $CuIn_{1-x}Ga_xSe_2$ thin films. *Solar Energy Materials and Solar Cells*, 58(4):375-385.
https://doi.org/10.1016/S0927-0248(99)00010-0

Hamakawa Y, 2012. Thin-film Solar Cells Next Generation Photovoltaics and Its Applications. Springer-Verlag Berlin Heidelberg, p.167.

Harati M, Jia J, Giffard K, et al., 2010. One-pot electrodeposition, characterization and photoactivity of stoichiometric copper indium gallium diselenide (CIGS) thin films for solar cells. *Physical Chemistry Chemical Physics*, 12(46):15282-15290.
https://doi.org/10.1039/c0cp00586j

Izquierdo-Roca V, Saucedo E, Ruiz CM, et al., 2009. Raman scattering and structural analysis of electrodeposited $CuInSe_2$ and S-rich quaternary $CuIn(S,Se)_2$ semiconductors for solar cells. *Physica Status Solidi (a)*, 206(5):1001-1004.
https://doi.org/10.1002/pssa.200881239

Jackson P, Hariskos D, Wuerz R, et al., 2014. Compositional investigation of potassium doped $Cu(In,Ga)Se_2$ solar cells with efficiencies up to 20.8%. *Physica Status Solidi (RRL)-Rapid Research Letters*, 8(3):219-222.
https://doi.org/10.1002/pssr.201409040

Jiang F, Feng J, 2006. Effect of temperature on selenization process of metallic Cu-In alloy precursors. *Thin Solid Films*, 515(4):1950-1955.
https://doi.org/10.1016/j.tsf.2006.07.154

Karg F, Probst V, Harms H, et al., 1993. Novel rapid-thermal-processing for CIS thin-film solar cells. Conference Record of the 23rd IEEE Photovoltaic Specialists Conference, p.441-446.

Kemell M, Ritala M, Saloniemi H, et al., 2000. One-step electrodeposition of $Cu_{2-x}Se$ and $CuInSe_2$ thin films by the induced co-deposition mechanism. *Journal of the Electrochemical Society*, 147(3):1080-1087.
https://doi.org/10.1149/1.1393317

Lakshmikumar ST, Rastogi AC, 1996. Phase evolution in low-pressure Se vapor selenization of evaporated Cu/In bilayer precursors. *Journal of Applied Physics*, 79(7):3585-3591.
https://doi.org/10.1063/1.361411

Lincot D, Guillemoles JF, Taunier S, et al., 2004. Chalcopyrite thin film solar cells by electrodeposition. *Solar Energy*, 77(6):725-737.
https://doi.org/10.1016/j.solener.2004.05.024

Malaquias JC, Steichen M, Dale PJ, 2015. One-step electrodeposition of metal precursors from a deep eutectic solvent for $Cu(In,Ga)Se_2$ thin film solar cells. *Electrochimica Acta*, 151:150-156.
https://doi.org/10.1016/j.electacta.2014.11.089

Mise T, Nakada T, 2009. Microstructural properties of $(In,Ga)_2Se_3$ precursor layers for efficient cigs thin-film solar cells. *Solar Energy Materials and Solar Cells*, 93(6-7):1000-1003.
https://doi.org/10.1016/j.solmat.2008.11.028

Panicker MPR, Knaster M, Kroger FA, 1978. Cathodic deposition of CdTe from aqueous-electrolytes. *Journal of the Electrochemical Society*, 125(4):566-572.
https://doi.org/10.1149/1.2131499

Powalla M, Voorwinden G, Hariskos D, et al., 2009. Highly efficient CIS solar cells and modules made by the co-evaporation process. *Thin Solid Films*, 517(7):2111-2114.
https://doi.org/10.1016/j.tsf.2008.10.126

Rau U, Schock HW, 1999. Electronic properties of $Cu(In,Ga)Se_2$ heterojunction solar cells–recent achievements, current understanding, and future challenges. *Applied Physics A: Materials Science & Processing*, 69(2):131-147.
https://doi.org/10.1007/s003390050984

Saji VS, Choi IH, Lee CW, 2011. Progress in electrodeposited absorber layer for $CuIn_{(1-x)}Ga_xSe_2$ (CIGS) solar cells. *Solar Energy*, 85(11):2666-2678.
https://doi.org/10.1016/j.solener.2011.08.003

Sebastian PJ, Calixto ME, Bhattacharya RN, et al., 1999. CIS and CIGS based photovoltaic structures developed from electrodeposited precursors. *Solar Energy Materials and Solar Cells*, 59(1-2):125-135.
https://doi.org/10.1016/S0927-0248(99)00037-9

Witte W, Kniese R, Eicke A, et al., 2006. Influence of the GA content on the $Mo/Cu(In,Ga)Se_2$ interface formation. Conference Record of the IEEE 4th World Conference on Photovoltaic Energy Conversion, p.553-556.
https://doi.org/10.1109/WCPEC.2006.279515

Witte W, Kniese R, Powalla M, 2008. Raman investigations of $Cu(In,Ga)Se_2$ thin films with various copper contents. *Thin Solid Films*, 517(2):867-869.
https://doi.org/10.1016/j.tsf.2008.07.011

Yamanaka S, Tanda M, Nakada N, et al., 1991. Study of $CuInSe_2$ formation kinetics in the selenization process by Raman spectroscopy. *Japanese Journal of Applied Physics*, 30(Part 1, No. 3):442-446.
https://doi.org/10.1143/JJAP.30.442

Yeh MH, Ho SJ, Chen GH, et al., 2016. Toward low-cost large-area CIGS thin film III: effect of Se concentration on crystal growth and defect formation of sequentially electrodeposited CIGS thin films. *Solar Energy*, 132:547-557.
https://doi.org/10.1016/j.solener.2016.03.029

Zhang HX, Hong RJ, 2016. CIGS absorbing layers prepared by RF magnetron sputtering from a single quaternary target. *Ceramics International*, 42(13):14543-14547.
https://doi.org/10.1016/j.ceramint.2016.06.067

Zhang Z, Li J, Wang M, et al., 2010. Influence of annealing conditions on the structure and compositions of electrodeposited $CuInSe_2$ films. *Solid State Communications*, 150(47-48):2346-2349.
https://doi.org/10.1016/j.ssc.2010.09.048

中文概要

题　目：退火条件对电沉积制备铜铟镓硒薄膜品质的影响

目　的：退火条件直接影响着电沉积制备的铜铟镓硒薄膜品质，而薄膜品质决定着最终得到器件的转换效率。本实验在不同退火条件下对薄膜进行处理，得出退火条件对薄膜各项表征指标的影响规律，并根据观察到的规律改善退火工艺，以提高铜铟镓硒薄膜品质。

创新点：目前利用水溶液电沉积制备的铜铟镓硒薄膜太阳能电池转换效率不高，而退火是制作此电池的关键步骤之一。本文研究了退火温度和升温速率对薄膜品质的影响，分析其可能原因及退火过程发生的反应，并制备出了理想的高品质薄膜。

方　法：1. 在水溶液中利用电沉积法制备出铜铟镓硒薄膜前驱体。2. 对前驱体进行退火处理，并针对不同的样品采用不同的退火温度和升温速率。3. 利用 X 射线衍射（XRD）、拉曼光谱（Raman）、扫描电子显微镜（SEM）、X 射线荧光光谱（XRF）对薄膜进行表征，分析不同退火条件对结果的影响规律。

结　论：1. 退火温度的影响：退火温度由 450 °C 升高到 580 °C 时，得到的薄膜结晶性越来越好，晶粒边界越来越不明显，Cu/(In+Ga)的比例逐渐升高，说明高温下（≥450 °C）金属铟和镓较易挥发；实验中还发现 Cu-Se 化合物的总含量随退火温度的升高而降低。2. 升温速率的影响：退火速率越高，薄膜结晶性越好；快速升温时薄膜中 Cu/(In+Ga) 的比例略低于慢速升温时的样品，而 Ga/(In+Ga) 的比例几乎不变，说明快速升温可以减少 In 和 Ga 的挥发。

关键词：铜铟镓硒薄膜；电沉积；退火条件；拉曼光谱